Microstructure and Fracture Behavior of Polypropylene/ Barium Sulfate Composites

Ke Wang,[1,2,3]* Jingshen Wu,[1] Hanmin Zeng[2,3]

[1]*Department of Mechanical Engineering, Hong Kong University of Science and Technology, Clear Water Bay, Kowloon, Hong Kong*
[2]*Key Laboratory of Polymeric Composite & Functional Materials, The Ministry of Education of China, Guangzhou, China*
[3]*Institute of Materials Science, Zhongshan University, Guangzhou, China*

Received 22 April 2004; accepted 19 February 2005
DOI 10.1002/app.22596
Published online in Wiley InterScience (www.interscience.wiley.com).

ABSTRACT: The microstructure, mechanical properties, and fracture behavior of polypropylene (PP)/barium sulfate ($BaSO_4$) composites were studied. Four composite samples with different PP-$BaSO_4$ interface were prepared by treating the filler with different modifiers. The fracture behavior of the composites under different strain rates was studied by means of Charpy impact tests and essential work of fracture (EWF) tests. It is shown that a moderate interfacial adhesion is favorable for toughening, which ensures that the particles transfer the stress and stabilizes the cracks at the primary stage of the deformation, and satisfies the stress conditions of plastic deformation for matrix ligaments subsequently *via* debonding. Very strong interfacial adhesion is not favorable for toughness, especially under high strain rate, because the debonding-cavitation process may be delayed and the plastic deformation of matrix may be restrained. © 2005 Wiley Periodicals, Inc. J Appl Polym Sci 99: 1207–1213, 2006

Key words: polypropylene; barium sulfate; inorganic particles; toughness; interface

INTRODUCTION

Inorganic fillers have been introduced into polymers to reduce the cost, improve the stiffness and dimension stability. Generally, the addition of inorganic fillers has an embrittling effect on polymers and results in a significant decrease of toughness. However, it was shown[1–6] that, in some filled polymer systems, such as polypropylene (PP)/calcium carbonate ($CaCO_3$) and high-density polyethylene (HDPE)/$CaCO_3$ composites, polymers can be toughened and reinforced simultaneously with the addition of rigid inorganic particles. Based on the theories of fracture mechanics, it has been demonstrated[4–6] that the toughening mechanism involves several steps, including stress concentration around filler particles, debonding between matrix and particles, transition of stress states ahead the crack tip from plane strain to plane stress, shear yielding of the matrix ligaments between particles and massive yield of matrix, etc.

The polymer–filler interfacial interaction has been generally suggested to be one of the most important factors controlling the mechanical properties of composites. Low toughness is frequently attributed to the weak interfacial bonding and poor filler dispersion.[2,6–8] Interfacial modifiers, such as stearates, silanes, titanates, and grafted copolymers, are frequently used in filled polymer systems to adjust polymer–filler interaction. Proper interfacial modification can reduce the aggregation of filler particles. It also leads to a better dispersion of particles in polymer matrix, and strengthens the polymer–filler adhesion. Accordingly, the debonding mechanisms and failure behavior of the composites are modified.[6]

On the other hand, crystalline morphology of semicrystalline polymer matrix is also an important factor that strongly influences the properties of filled polymer systems.[5,9] The modified polymer–filler interfacial interaction can promote the adsorption of polymer molecules onto filler surface and leads to changes in the nucleating ability of the fillers[10–12] and the crystalline morphology of the matrix.[9] In some cases, these changes are crucial for toughening. Bartczek *et al.*[4] studied the toughening mechanisms for the HDPE/$CaCO_3$ particle composites and found that the fracture toughness of the composites would be high if debonding between the $CaCO_3$ particles and the matrix occurred and interparticle ligament thickness was below a critical value. The authors further suggested that the

*Present address: Molecular and Performance Materials Cluster, Institute of Materials Research and Engineering, 3 Research Link, Singapore.
Correspondence to: Ke Wang (k-wang@imre.a-star.edu.sg).
Contract grant sponsor: Research Grant Council (RGC) of Hong Kong; contrct grant number: HKUST 6105/97E.

interparticle ligaments in the HDPE/$CaCO_3$ composite possess a highly ordered lamellar structure, which has a reduced plastic resistance in certain orientations. When this structure percolates throughout the composite, the overall plastic resistance of the composites is markedly reduced, leading to a large unhindered plastic extension in the matrix ligaments, hence, a greatly improved toughness. More recently, Chan et al.[5] found that nanoscale $CaCO_3$ particle is an effective nucleating agent for PP, which causes the absence of detectable spherulites. The authors believed that reduction in the size of the spherulites is one of the main factors contributing to high toughness of the PP/nano-scale $CaCO_3$ composites.

Up to now, the most successful inorganic particle toughening systems are PP/$CaCO_3$ and HDPE/$CaCO_3$ composites. It is obvious that more successful systems are needed to give deeper understanding of the toughening mechanisms. Recently, a group of PP/barium sulfate ($BaSO_4$) composites with different interfacial properties was prepared by applying different interfacial modifications. Preliminary works[13–15] have shown that $BaSO_4$ particles are effective in nucleating the crystallization of PP, promoting the formation of small and less perfect PP spherulites, and reinforcing and toughening PP simultaneously. In this paper, the microstructure and fracture behavior of the PP/$BaSO_4$ composites are studied and the toughening mechanisms are discussed.

EXPERIMENTAL

Materials

The PP homopolymer (F401, melt flow rate = 2.5 g/min) was manufactured by Guangzhou Petrochemical Company, China. The $BaSO_4$ powder with a weight average particle size of 1.29 μm (polydispersity index = 1.645) was provided by Qingdao Chemical Factory and was calcined at 400°C for 6 h before use to remove contaminants. The silane coupling agent (AMPTES, $(C_2H_5O)_3SiC_3H_6NH_2$) and stearic acid were purchased from Gaixian chemical factory. The PP-*graft*-maleic anhydride (PP-*g*-MAH) copolymer was prepared in our laboratory via melt reactive extrusion procedure. The MAH content is ~0.66 wt %.

Sample preparation

A two-step mixing process was employed to produce the PP/$BaSO_4$ composites with different type of interface. In the first step, masterbatches with 80 wt % of $BaSO_4$ filler were prepared. The $BaSO_4$ powder pretreated with/without coupling agent was mixed with a carrier resin (PP or PP-*g*-MAH) in a two-roll mill at 170–180°C for 15 min and then granulated. The detail of the $BaSO_4$ surface treatment, composition, and designation of the masterbatches are listed in Table I.

TABLE I
Composition of the Masterbatches

Designation	Carrier polymer	Coupling agent
M-0	PP	None
M-SA	PP	Stearic acid (1 wt %)[a]
M-SI	PP	AMPTAS (1 wt %)[a]
M-MAH	PP-*g*-MAH	None

[a] Based on $BaSO_4$.

In the second step, the final composites were obtained by compounding each of the masterbatches with virgin PP in a corotating twin-screw extruder at 200–220°C and 200 rpm. The resultant composites are designated hereafter as C-0 for PP/M-0, C-SA for PP/M-SA, C-SI for PP/M-SI, and C-MAH for PP/M-MAH, respectively. All samples contained 24 wt % of $BaSO_4$. For comparison, a control sample, named as neat PP, was prepared by a single extrusion of the virgin PP without fillers, under the same condition. Specimens were injection-molded (Chen Hsong JM88MK-IIIC) at barrel temperatures of 210°C.

To observe the dispersion of the particles, injection-molded samples were immersed in liquid nitrogen for 5 min, and then hammered to break. The cryo-fractured surfaces were sputtered with gold and observed with a JEOL 6300 scanning electron microscopy (SEM).

Mechanical testing

The tensile tests were conducted with dog-bone bars (ASTM D-638, type III specimen) at room temperature with a Sintech D/10 MTS tester at a crosshead rate of 10 mm/min. For impact testing, notches with a root radius of 0.254 mm and a depth of 2.54 mm were cut on one side of the specimen (ASTM D 256 specimen, 125× 12.7× 3 mm^3) with a Ceast notching cutter. Charpy impact tests were conducted on an instrumented impact tester (RADMANA ITR-2000) at room temperature. The pendulum speed at impact was 1.34 m/s.

EWF method

The fracture toughness was characterized with EWF method. The details of the method can be found in Ref. 17. According to the theory of EWF,[16,17] fracture process and the plastic deformation take place in two different regions, process zone and plastic zone, respectively. The total work done for fracture is the sum of the energy dissipated in both process zone and plastic zone, which can be expressed as:

$$W_f = W_e + W_p \quad (1)$$

where W_f is the total work of fracture, W_e is the EWF, which is the energy dissipated on the fracture area of process zone, and W_p is the nonessential work, which is the energy dissipated in the plastic zone. Considering that W_e is surface related, whereas W_p is volume related, W_f can be given by the related specific work terms:

$$W_f = w_e lt + w_p \beta l^2 t \quad (2)$$

$$w_f = \frac{W_f}{lt} = w_e + w_p \beta l \quad (3)$$

where w_f is the specific total fracture work, w_e is specific EWF, β is a shape factor plastic zone, w_p is specific nonessential work of fracture, t is the thickness of specimen, l is the ligament length. According to eq. (3), a linear relation is obtained as the specific work of fracture (w_f) is plotted against the ligament length, l. The w_e and $w_p\beta$ can be determined by the interception and the slope of the plot, respectively.

Double-edge notched tension (DENT) specimens with dimensions of 157× 39× 3 mm^3 were used (Fig. 1). The notches were made by first cutting with band saw, followed by sharpening with a fresh razor blade. The ligament length varied from 5 mm to 25 mm. The experiments of the specimens were carried out on a Sintech D/10 MTS at a crosshead speed of 5 mm/min. The exact ligament length was measured with a measuring microscope (Topcon TMM-13OZ). The fracture surfaces were coated with gold and observed with a JEOL 6300 SEM.

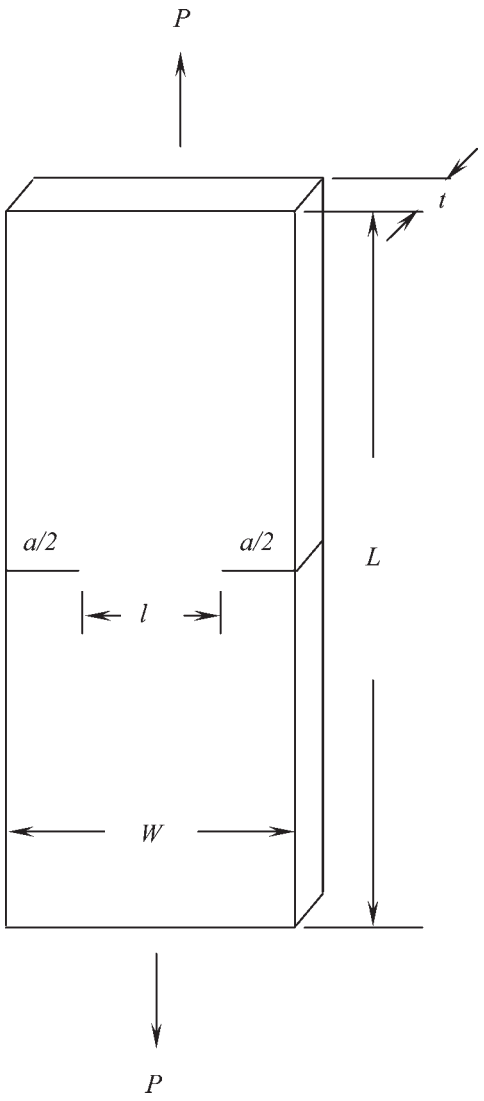

Figure 1 Double-edge notched tension (DENT) specimens used for fracture experiments.

RESULTS

Microstructure

The SEM image of the cryo-fractured surfaces of C-0, C-SA, C-SI, and C-MAH are shown in Figures 2(A)–2(D), respectively. In Figure 2(A), large $BaSO_4$ agglomerates (indicated by arrows) are observed on the surface of the C-0, and many particles were pulled out from the matrix, indicating that plain $BaSO_4$ particles are not well dispersed and the interfacial bonding between particles and matrix is weak. When the fillers were treated with stearic acid, the particle dispersion is improved although there are still some aggregates, as indicated by arrows in Figure 2(B). For the C-SI, in which the fillers were coated with silane, the dispersion of particles is improved considerably and few particles are pulled out [Fig. 2(C)]. Good dispersion of the particles and strong interfacial adhesion are achieved when the interface was modified with PP-*g*-MAH. As can be seen in Figure 2(D), the filler particles are firmly embedded in the matrix and very few pulling out or debonding can be seen.

The crystalline structure of the injection-molded samples has been studied[14] by means of wide-angle X-ray diffraction (WAXD) measurements. It has been shown[14] that α-form crystallites are dominant in the neat-PP and all the composites, while very little β-form crystallites were detected in the composite samples. The overall crystallinity (X_c%) values calculated from WAXD data are listed in Table II. The PP matrix in the C-SA has the lowest crystallinity among the samples. In the C-MAH and the C-SI, PP matrix has higher crystallinity than neat PP. The C-0 exhibits similar crystallinity as neat PP. The content of β-form PP crystallites in the composites is lower than 2%, which is not enough to affect the mechanical property of the composites.

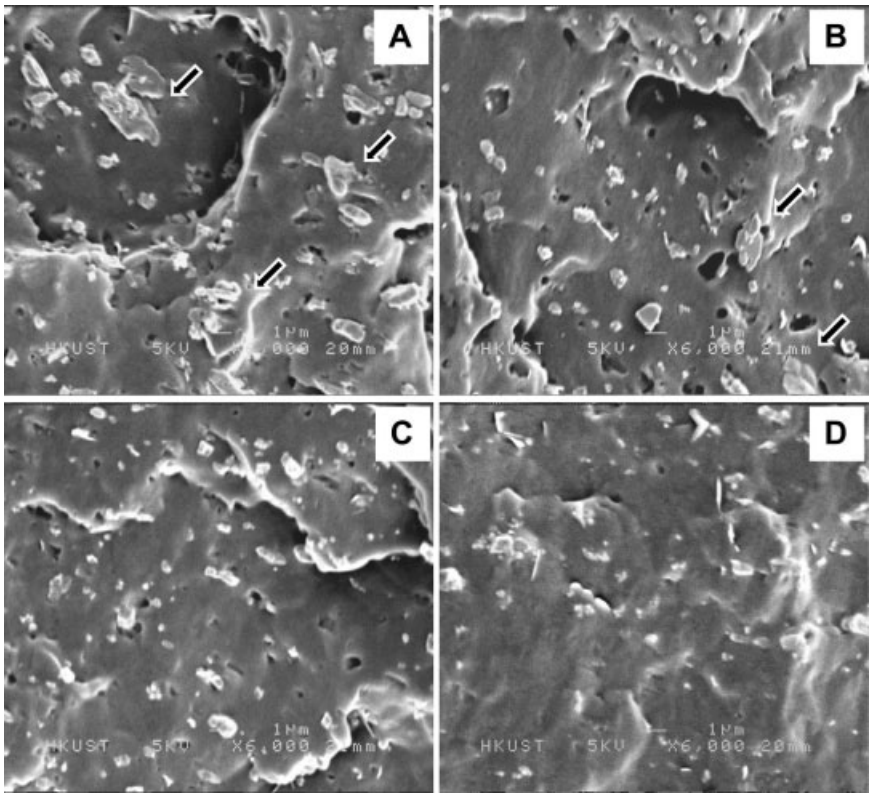

Figure 2 SEM micrographs of the cryo-fractured surfaces of PP/$BaSO_4$ composites.

Mechanical properties

The yield stress, Young's modulus, and impact strength of neat PP and the PP/$BaSO_4$ composites are collected in Table II. The incorporation of 24 wt % $BaSO_4$ particles results in a slight decrease in yield stress and a remarkable increase in Young's modulus. It is notable that the values of yield stress and Young's modulus are dependent on the interfacial modifications. The C-MAH and the C-SI, in which the interfaces were modified with PP-*g*-MAH and silane, have higher yield stress and Young's modulus than those without modification (C-0) or modified with stearic acid (C-SA), showing pronounced reinforcements. It is obvious that this phenomenon can be attributed to stronger interfacial adhesion and higher crystallinity of PP matrix in these composites.

The neat PP exhibits low impact strength (2.66 kJ/m^2) because of its notch-sensitive nature. The incorporation of $BaSO_4$ particles leads to considerable increases in impact strength relative to neat PP. The composite containing stearic acid treated $BaSO_4$ particles (C-SA) exhibits particularly good resistance to impact failure and the highest toughness among the composites (5.40 kJ/m^2), which is double that of neat PP.

Fracture toughness

Figure 3 shows typical load-displacement curves of the neat PP and PP/$BaSO_4$ composites. Obviously, the fracture behavior of the DENT specimens is dependent on the nature of the materials. The neat PP shows a quite brittle fracture manner. Only slightly plastic deformation and small stress whiting zone near the tip of the notches can be observed. This phenomenon indicates that the specimen is too thick to ensure a plane-stress condition for the neat PP. All PP/$BaSO_4$ composites, however, are very ductile, which exhibit extensive yielding and necking. Crack starts at the sharpened notches after complete yielding of the processing zone and propagates in a stable manner. For the same material, the shape of the load-displacement curve is similar and independent of ligament length.

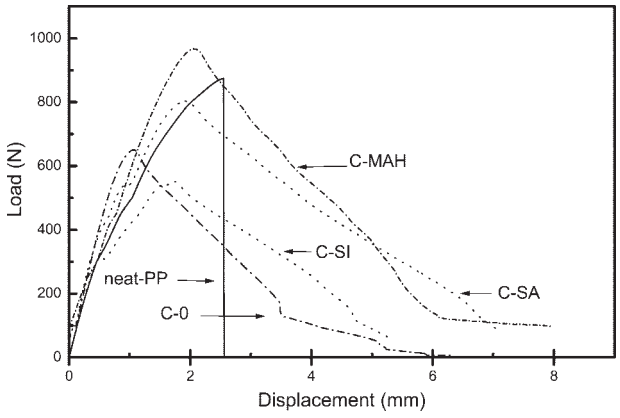

Figure 3 Typical load-displacement curves of neat-PP and PP/$BaSO_4$ composites obtained with DENT specimens.

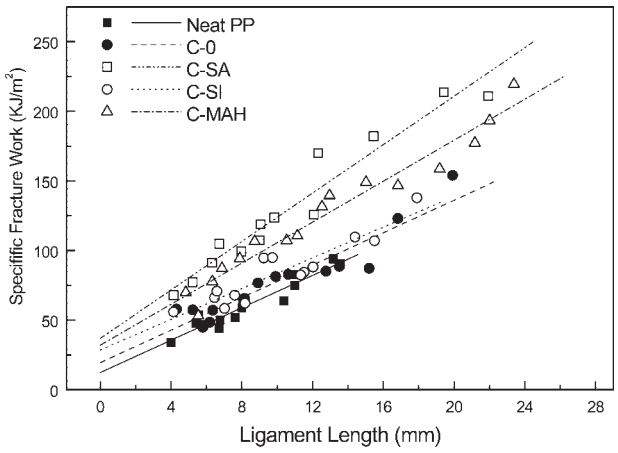

Figure 4 Plots of specific fracture work, w_f, against ligament length, l, for PP/$BaSO_4$ composites.

The plots of specific total work of fracture, w_f, against specimen ligament length, l, for the neat PP and the PP/$BaSO_4$ composites are shown in Figure 4. The results of the plots indicated that the w_f values increased proportionally to the ligament length and very good linear regression coefficients were obtained. From the interception and the slope of the regression line, the w_e and βw_p were determined and summarized in Table II. For the neat PP, a w_e value of 12.4 kJ/m^2 was obtained despite the specimen geometry is hardly meet the requirement of EMF method.[18–20] This value is very close to the recently reported EWF values of the order of 15 kJ/m^2 for neat PP.[20] The incorporation of nontreated $BaSO_4$ particles led to significant increase (~57%) of the w_e value (from 12.4 kJ/m^2 to 19.5 kJ/m^2). With interfacial modification, the w_e was further improved with respect to the neat PP. The w_e of the C-SA and the C-MAH reached +200% and +158% of the original value of the PP, respectively. At the same time, significant increase (+50% and +28%, respectively) of the βw_p values were also observed for the C-SA and the C-MAH. These EWF results show that the interfacial modification with stearic acid and PP-*g*-MAH not only led to a substantial improvement of fracture toughness, it also led to a considerable increase in the plastic work dissipation.

Figure 5 presents the morphology of the fracture surfaces of the neat PP and the composites. For the neat PP [Fig. 5(A)], some shear-type dimples are observed, indicating localized shear deformation. For the composite samples, the fracture surfaces are similar to each other, which are dominated by highly plastically deformed zone filled with voids. The matrix ligaments between these voids are stretched and deformed extensively. The morphology characteristics of the fracture surface of the composites reveal that a cavitation-induced shear deformation[4,21,22] is most probably the dominant energy-dissipation event responsible for the high toughness of the composites.

To give a clear elucidation of the toughening mechanisms, central section of the C-SA tensile bars after different extent of extension was cut, coated with gold, and observed under SEM. At the beginning of the deformation [Fig. 6(A)], $BaSO_4$ particles serve as stress concentrators in the composites, stress concentration occurs at the poles of the particles because there are some extent of interfacial adhesion between the matrix and the particles; with the progress of deformation, debonding starts at the poles of the particles [Fig. 6(B)], the matrix around the voids stretches and the voids grow parallel to the direction of load [Fig. 6(C)]. After debonding, the plastic constraint stresses were relieved and the stress-state of the matrix at the crack-tip can convert from a plane-strain condition to a plane-stress condition if the ligament thickness between the neighboring rigid particles is less than the critical value of the matrix polymer. Consequently, the matrix ligament between the voids undergoes extensive plastic deformation, as indicated by the arrow [Fig. 6(D)]. This process absorbs a large amount of energy, resulting in enhanced fracture toughness.[23]

DISCUSSION

It is notable that the effect of interfacial modification on the relative toughness of PP/$BaSO_4$ composites is related to strain rate. For high-speed impact tests, the

TABLE II
Crystallinity, Tensile Properties, Impact Strength, and EWF Parameters of the Neat PP and the PP/$BaSO_4$ Composites[a]

Sample code	X_c (%)[b]	Yield strength (MPa)	Young's modulus (GPa)	Impact strength (kJ/m^2)	w_e (kJ/m^2)	βw_p (mJ/m^3)	R
Neat PP	46.4	29.9 (0.50)	1.19 (0.055)	2.7 (0.49)	12.4	5.8	0.9614
C-0	47.1	27.7 (0.29)	1.78 (0.042)	4.0 (0.40)	19.5	5.8	0.9381
C-SA	44.5	27.5 (0.20)	1.73 (0.068)	5.4 (0.52)	36.9	8.7	0.9703
C-SI	50.3	28.3 (0.22)	1.81 (0.045)	4.5 (0.29)	28.5	5.5	0.9251
C-MAH	52.9	28.7 (0.25)	1.96 (0.068)	3.7 (0.60)	32.0	7.4	0.9775

[a] Standard deviation values are given in parentheses.
[b] From Ref. [14].

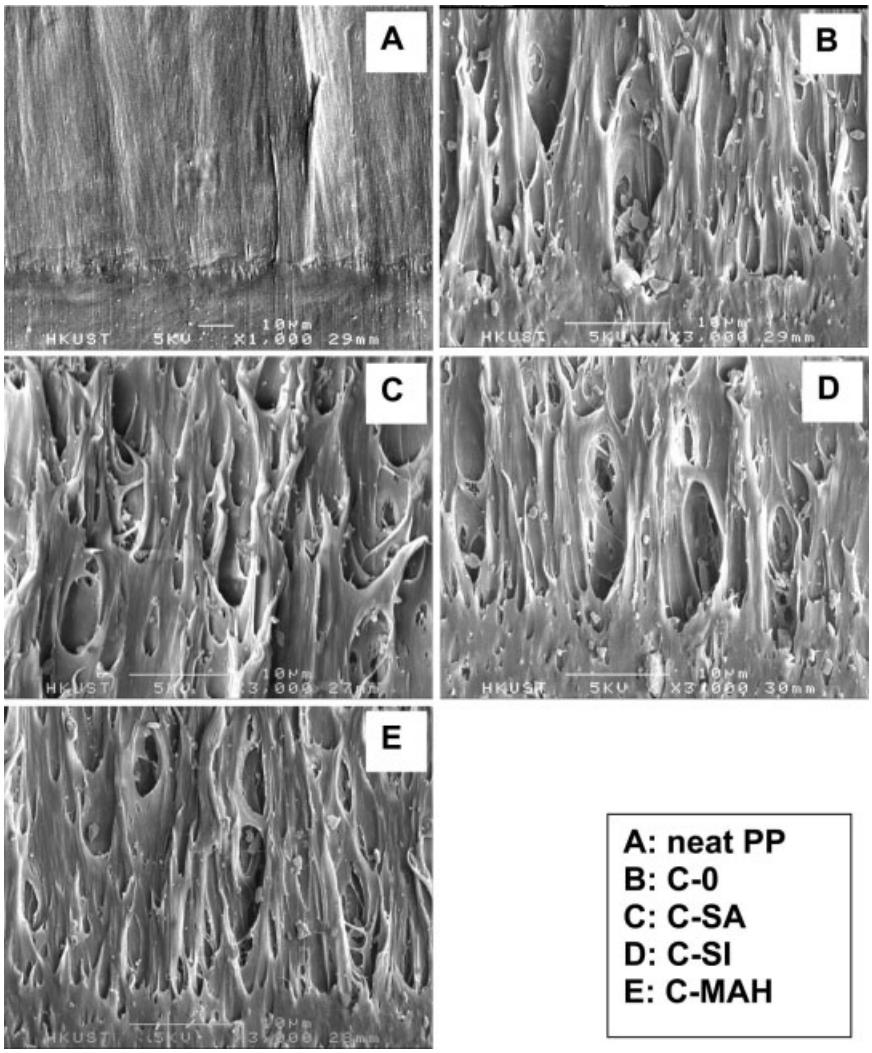

Figure 5 SEM photographs taken from the fracture surface of neat PP and PP/$BaSO_4$ composites.

impact strength of the C-0 is higher than that of C-MAH, whereas in low speed EMF tests, the sequence revised. It is obvious that debonding-cavitation is a time-dependent process. At a high strain rate, the loading time is short and the debonding-cavitation process may be delayed if the interfacial adhesion is too strong, as in the C-MAH. Consequently, few filler particles were debonded before catastrophic failure took place. The zones satisfying the condition of plane-stress in the C-MAH are less than that in other composites and the volume of the plastic deformation zone in the C-MAH is limited. In the EWF tests, however, the strain rate is low enough for all samples to undergo debonding-cavitation and plastic deformation. In the C-0, the dispersion of filler particles in the matrix is poor and the interfacial adhesion between polymer and filler is weak, so that they may nucleate plenty of fatal cracks and show low ability of crack resistance, which in turn resulted in low toughness. Thus, a good dispersion of fillers and a moderate interfacial adhesion, like in the C-SA, are favorable for toughening, which ensures that the particles transfer the stress and stabilizes the cracks at the primary stage of the deformation, and controls the debonding of the particles at proper opportunities to satisfy the stress conditions of plastic deformation for matrix ligaments.

The characteristic of the matrix is also responsible for the toughening. For crystalline polymers, extensive studies have demonstrated that lower crystallinity, smaller spherulite size, and less perfection of crystallites are favorable to ductile deformation and low yield stress.[24–29] Therefore, it is believed that the changes in the crystalline structure of the PP matrix due to the incorporation of $BaSO_4$ particles are also important factors determining the toughening effects. According to the foregoing, the C-SA has the lowest crystallinity among the composites. This may be one of the main reasons that the C-SA exhibits the highest toughness.

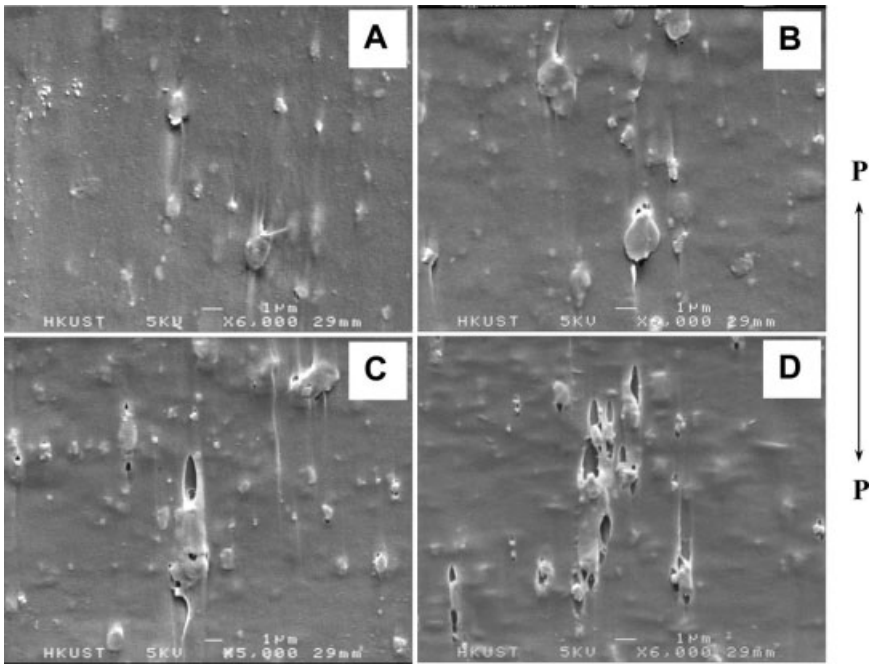

Figure 6 SEM micrographs of the surface of C-SA after being stretched to different strains. (A) 10%, (B) 18%, (C) 30%, (D) 40%.

CONCLUSIONS

The incorporation of $BaSO_4$ into PP leads to higher modulus and toughness. The particles act as stress concentrators in the matrix and promote cavitation at the matrix-particle boundary and in turn initiate massive large-scale plastic deformation of matrix. Interfacial modification improves particle dispersion and interfacial adhesion, and affects the crystallization of PP matrix to form small and less perfect spherulites.[13,14] In the present PP/$BaSO_4$ systems, stearic acid renders a moderate interfacial adhesion, which promotes the plastic deformation of matrix and leads to substantial improvement of fracture toughness. Very strong interfacial adhesion is not favorable for toughness, especially under high strain rate, because the debonding-cavitation process may be delayed and the plastic deformation of matrix maybe restrained. On the other hand, lower crystallinity of the PP matrix facilitates shear yielding. This is most likely the reason why the stearic acid modified system (C-SA) exhibits highest toughness among the PP/$BaSO_4$ composites studied in this work.

Technical supports from the Advanced Engineering Materials Facilities (AEMF) and the Materials Characterization and Preparation Facilities (MCPF) at the Hong Kong University of Science and Technology (HKUST) are also acknowledged.

References

1. Nezbenova, E.; Ponesicky, J.; Sova, M. Acta Polym 1990, 41, 36.
2. Fu, Q.; Wang, G.; Liu C. Polymer 1995, 36, 2397.
3. Li, D.; Zheng, W.; Qi, Z. J Mater Sci 1994, 29, 3754.
4. Bartczak, Z.; Argon, A. S.; Cohen, R. E.; Weinberg, M. Polymer 1999, 40, 2347.
5. Chan, C. M.; Wu, J. S.; Li, J. X.; Cheung, Y. K. Polymer 2002, 43, 2981.
6. Zuiderduin, W. C.; Westzaan, C.; Huetink, J.; Gaymans, R. J. Polymer 2003, 44, 261.
7. Hancock, M.; Tremayne, P.; Rosevear, D. J. J Polym Sci 1980, 18, 3211.
8. Hornsby, P. R.; Watson, C. L. J Mater Sci 1995, 30, 5347.
9. McGenity, P. M.; Hooper, J. J.; Paynter, C. D.; Riley, A. M.; Nutbeem, C.; Elton, N. J.; Adams, J. M. Polymer 1992, 33, 5215.
10. Velasco, J. I.; de Saja, J. A.; Martinez, A. B. J Appl Polym Sci 1996, 61, 125.
11. Alonso, M.; Velasco, J. I.; de Saja, J. A. Eur Polym J 1997, 33, 255.
12. Liu, Z.; Gilbert, M. J Appl Polym Sci 1996, 59, 1087.
13. Wang, K.; Wu, J. S.; Zeng, H. M. Eur Polym J 2003, 39, 1647.
14. Wang, K.; Wu, J. S.; Ye, L.; Zeng, H. M. Composite A 2003, 34, 1199.
15. Wang K.; Wu, J. S.; Zeng H. M. Polym Int 2004, 53, 838.
16. Wu, J. S.; Mai, Y. -W. Polym Eng Sci 1996, 36, 2275.
17. Mai, Y. W.; Cotterell, B. Int J Fract 1984, 24, 229.
18. Tiong, S. C.; Xu, S. A.; Li, R. K. Y.; Mai, Y. W. Polymer Int 2002, 51, 1248.
19. Maspoch, M. L.; Gamez-Perez, J.; Gordillo, A.; Sanchez-Soto, M.; Velasco, J. I. Polymer 2002, 43, 4177.
20. Bureau, M. N.; Perrin-Sarazin, F.; Ton-That, M. -T. Polymer Eng Sci 2004, 44, 1142.
21. Wu, J. S.; Mai, Y.W.; Yee, A. F. J Mater Sci 1994, 29, 4510.
22. Wu, J. S.; Yu, D. M.; Mai, Y. W.; Yee, A. F. J Mater Sci 2000, 35, 307.
23. Kim, G. –M.; Michler, G. H. Polymer 1998, 39, 5699.
24. Schultz, J. M. Polym Eng Sci 1984, 24, 770.
25. van der Wal, A.; Mulder, J. J.; Gaymans, R. J. Polymer 1998, 39, 5477.
26. Perkins, W. G. Polym Eng Sci 1999, 39, 2445.
27. Friedrich, K. Prog Colloid Polym Sci 1978, 64, 103.
28. Way, J. L.; Atkinson, J. R.; Nutting, J. J Mater Sci 1974, 9, 293.
29. Lustiger, A.; Marzinsky, C. N.; Mueller, R. R. J Polym Sci Part B: Polym Phys 1998, 36, 2047.